Charge models for electron spectroscopy of disordered alloys

T. L. Underwood, P. D. Lane, N. Miller, R. Stoker, and R. J. Cole
SUPA, School of Physics, University of Edinburgh, Edinburgh EH9 3JZ, United Kingdom
(Received 19 August 2008; revised manuscript received 17 December 2008; published 26 January 2009)

Disorder broadening can be observed in the core photoelectron spectra of metallic alloys. This effect can be simulated using a model in which site charges are assumed to be proportional to number of "unlike" atoms in the nearest-neighbor shell. This linear charge model (LCM) gives a sensible description of the variation in Madelung potential in disordered alloys and is reasonably self-consistent but significantly overestimates core disorder broadening as compared with *ab initio* core eigenvalue calculations and experimental core-level binding-energy measurements. Two generalizations of the LCM are investigated: an electronegativity model, in which charge is exchanged between unlike nearest neighbors in a nonlinear fashion, and a linear multishell model. Analytical and computational results are presented in each case and the implications for the analysis of core-level photoelectron spectra are discussed.

DOI: 10.1103/PhysRevB.79.024203 PACS number(s): 71.23.−k, 79.60.−i

I. INTRODUCTION

The Madelung energies of ordered arrays of charged balls explain the energetics and structural trends of ionic and partially ionic compounds,[1] but this model is not generally believed to be relevant to metallic alloys. Indeed there is no compelling definition of site charges in metallic systems, and given the availability of *ab initio* electronic structure methods one may infer that charge transfer is an unnecessary concept. However many metallic alloys form random substitutional systems whose description represents a rather demanding computational challenge. Traditionally the electronic structure of disordered binary systems has been treated using a mean-field framework, such as the coherent-potential approximation (CPA),[2–4] in which an A-type and a B-type atoms are embedded in a homogeneous medium whose properties are chosen to mimic those of the true disordered system as closely as possible. The CPA has proved extremely successful in describing a wide range of material properties.[5] There is a well-known problem, however. Since there is no information on the distribution of site charges about their conditionally averaged values, Q_A and Q_B, or their spatial distribution, the Madelung energy is implicitly neglected. Magri *et al.*[6] pointed out that the Madelung energy does not vanish if the net charge on a particular atom is determined by its *local* environment even if the site occupations are random. A model in which the charge on each atom is assumed to be linearly proportional to its number of unlike nearest neighbors,[6] referred here as the "linear charge model (LCM)," gives rise to a surprisingly large Madelung energy which has been shown to account for the structural stability of a number of compounds and alloys.[6–8] This early work stimulated a reassessment of the relevance of Madelung effects in metallic systems, and methods for their inclusion into CPA calculations have been devised,[9–11] as summarized in Ref. 5.

Electrostatics in disordered binary alloys have also been investigated experimentally using core-level photoelectron spectroscopy.[12] In particular Ref. 12 sought to answer a long-standing question: given that average core-level binding energies in metallic binary alloys vary by ~1 eV with global composition, should not variations in *local* composition give rise to a significant broadening of core-level spectra in disordered alloys? Reference 12 and subsequent studies[13–16] have shown that identification of core-level disorder broadening is just within the capability of the highest-resolution photoelectron spectrometers and that the effect has magnitude of a few tenths of eV. It was shown further that the LCM implies a core disorder broadening of similar magnitude, and indeed this conclusion has subsequently been drawn from *ab initio* electronic structure calculations.[17]

While the magnitude of the disorder broadening of core potentials has been established by experimental measurements, model calculations, and *ab initio* results, detailed comparisons for specific systems yielded only semiquantitative agreement.[16] Very recently Marten *et al.*[18] provided an explanation by demonstrating that disorder broadening in core hole relaxation energies (beyond the scope of the earlier *ab initio*[17] and model[12] calculations) can be as important as that in initial-state core potentials and that the two effects can either cancel or reinforce in photoelectron spectra. It is well known that the separation of initial-state and final-state effects in photoelectron spectroscopy can be aided by combination with the corresponding core Auger spectra,[19] and efforts in this direction have begun.[20,21] The discrepancies between *ab initio* and LCM predictions are also very much worth pursuing since such models can guide approximations employed in more sophisticated calculations, emphasize the main underlying concepts, and also provide a simple framework for analyzing experimental results.[22] In this context we re-examine the validity of the LCM and investigate the performance of its various generalizations with particular reference to recent computational results.[23–25]

II. Q-V RELATIONSHIP

In a system of charged balls the electrostatic potential in the core of site i is determined by the Madelung potential for that site plus an intra-atomic term,

$$V^i = V^i_{ia} + V^i_M = V^i_{ia} + F\sum_{j\neq i}\frac{Q^j}{R^{ij}} = V^i_{ia} + F\sum_{m\geq 1}\frac{Q_m}{R\rho_m}, \quad (1)$$

where R is the nearest-neighbor distance, $R\rho_m$ is the radius of the mth shell surrounding site i, Q^i is the charge on site i, and

 ©2009 The American Physical Society

Q_m is the total charge on sites in the mth shell. The constant F is omitted from subsequent equations for brevity. (It takes the value 14.4 when charges are measured in units of the proton charge, distances in angstrom, and potentials in volts.) Making the plausible assumption that the local charge resides at an effective radius of $R/2$ (i.e., $\rho_0=1/2$), the conditionally averaged core potentials can be written as

$$\langle V\rangle = \frac{\langle Q\rangle}{R}(2-\alpha_{\text{eff}}), \tag{2}$$

where α_{eff} is an effective Madelung constant. While the previous equation describes the *average* potential at A sites, the primary interest in this work is the *distribution* about that average. Adopting a strict single-site perspective with all A atoms having charge Q_A and all B atoms having charge Q_B, referred here as the "uniform charge assumption (UCA)," the average Madelung potential vanishes ($\alpha_{\text{eff}}=0$) due to global electroneutrality. The variance of V takes the form,

$$\sigma_V^2 = \left\langle \left(\sum_j \frac{Q^j}{R^j} \right)^2 \right\rangle = \left\langle \sum_j \left(\frac{Q^j}{R^j} \right)^2 \right\rangle = \frac{Q_0^2}{R^2} \frac{c_0}{1-c_0} \sum_m \frac{Z_m}{\rho_m^2}, \tag{3}$$

where Z_m is the number of sites in the mth shell and c_0 is the global concentration of the species found at the central site (shell zero). Since Z scales as ρ^2 the contribution to σ_V^2 from increasingly distant shells does not diminish and the variance is divergent, a prediction disproved by countless experimental x-ray photoemission studies of alloys. The distribution of site potentials implied by the UCA is not consistent with its own single-site nature.

It is clear that a reasonable description of electrostatics in disordered alloys requires a better description of site charges than that offered by the UCA. *Ab initio* electronic structure calculations using supercells containing hundreds of atoms[18,23,26] suggest that site charges take a continuous range of values and are linearly related to the corresponding Madelung potentials. This surprisingly simple relationship appears to be rather exact. Although currently no derivation has been given within the *ab initio framework*, the physics underlying these observations was illuminated by Pinski[27] using a Thomas-Fermi model. The linear Q-V_M effect is seen to result from the charge tracking the local Fermi level.[27] The results in Ref. 27 also allow rationalization of short-range and long-range Coulomb effects observed in *ab initio* calculations and explain the viability of simple charge models such as that[6] used previously to interpret experimental disorder broadening effects in core-level photoemission spectra. We now consider the extent to which such charge models reproduce linear Q-V_M behavior. This is done by complementing analytical results with numerical evaluation of Eq. (1) for a variety of clusters, typically containing $\sim 10^5$ sites, as described previously.[12,13,28]

III. CHARGE MODELS

A. Linear charge model

The charge model proposed by Magri *et al.*[6] has the form,

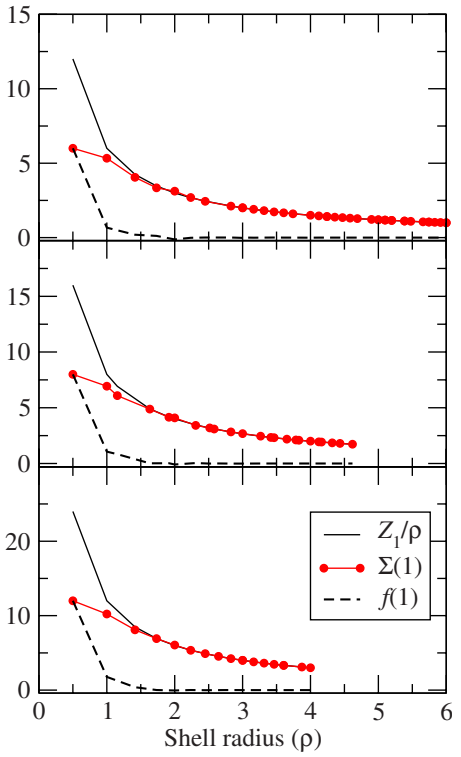

FIG. 1. (Color online) Variation in ρ of Z_1/ρ, $\Sigma(1)$, and $f(1)$ for the simple cubic (upper panel), body-centered-cubic (middle), and face-centered-cubic (lower panel) lattices.

$$Q^i = 2S_0\lambda_1 N_1, \tag{4}$$

where N_1 is the number of unlike neighbors in the first-neighbor shell, S_0 is the sign of the charge on site 0, and λ_1 sets the scale of the charges. It has been shown previously[13] that the resulting site potentials are given by

$$V(N_1,N_2,N_3,N_4,\ldots) = \frac{2\lambda_1 S_0}{R} \sum_{\alpha=0}^{\infty} f_\alpha(1)[Z_\alpha(1-c_0) - N_\alpha], \tag{5}$$

where

$$f_\alpha(n) = \frac{Z_n}{\rho_\alpha} - \Sigma_\alpha(n) = \frac{Z_n}{\rho_\alpha} - \sum_{m=0}^{\infty} \frac{K_\alpha^m(n)}{\rho_m} \tag{6}$$

and $K_\alpha^m(n)$ is the number of sites in the mth shell that are nth nearest neighbors of a site in the αth shell. It follows that the conditionally averaged potentials are

$$\langle V\rangle_{A(B)} = \frac{2\lambda_1 S_0}{R}(1-c_0)Z_1 = \frac{2\lambda_1 S_0}{R}\langle N_1\rangle_{A(B)} \tag{7}$$

with variance

$$\sigma_V^2 = \frac{4\lambda_1^2}{R^2} \sum_{\alpha=1}^{\infty} \sigma_{N_\alpha}^2 f_\alpha^2(1) = \frac{4\lambda_1^2}{R^2} c_0(1-c_0) \sum_{\alpha=1}^{\infty} f_\alpha^2(1) Z_\alpha. \tag{8}$$

$\Sigma(1)$ and Z_1/ρ versus ρ are shown in Fig. 1 for the face-centered-cubic (fcc), body-centered-cubic (bcc), and simple cubic (sc) lattices. Taylor expansion of $\Sigma(1)$ shows that $f(1)$

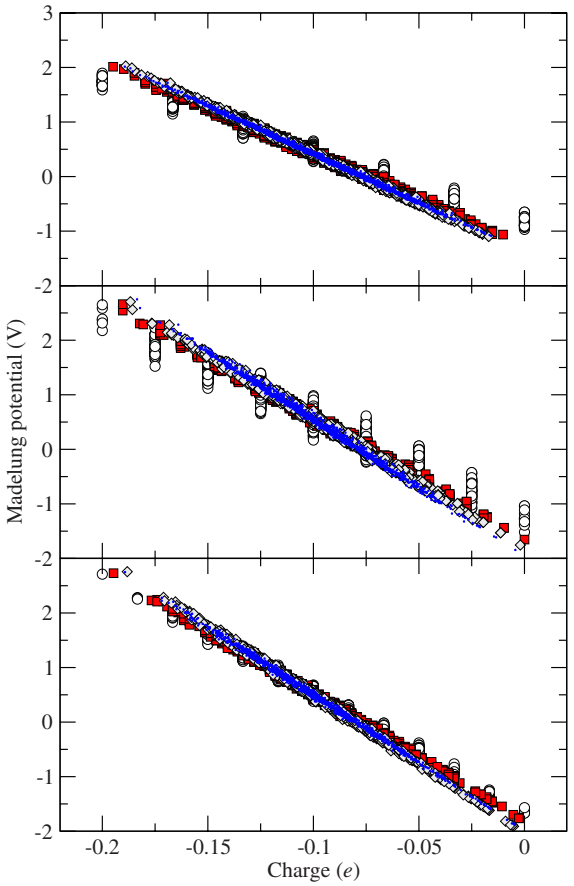

FIG. 2. (Color online) Madelung potential vs Q for the simple cubic (top), body-centered-cubic (middle), and the face-centered-cubic (lower panel) lattices, each populated randomly with equal numbers of A and B atoms. In each case the open circles correspond to the LCM data points. Red (dark gray) square, light gray diamond, and blue (black) dot data points correspond to the optimized multishell model with $\beta_{\max}=2,3,4$, respectively.

vanishes as ρ^{-5} for the lattices considered here. It follows that in each case σ_V is finite, is determined by composition variations in just the first few shells, and has magnitude smaller but comparable to $\langle V\rangle$. Since mean core-level shifts in metallic alloys are typically of order of 0.5 eV, the LCM predicts a core disorder broadening of a few tenths of eV. An effect of just this magnitude has been observed in a variety of fcc and bcc alloy systems,[12–16] suggesting that Magri's LCM provides a reasonable description of electrostatics in disordered alloys.

Plots of V_M^i against Q^i offer a more detailed test of the Magri charge model and such data are shown as circles in Fig. 2 for the face-centered-cubic, body-centered-cubic, and simple cubic lattices. Obviously the charges are quantized according to Eq. (4) rather than the continuous distribution of *ab initio* results, and the desired linear Q-V_M relation is reproduced only approximately. It has been shown previously[12,13,28] that $\langle V(N_1)\rangle$ (i.e., the conditionally averaged potential at sites with a particular N_1) is linear in N_1 (and hence Q) and that the scatter observed in Fig. 2 arises due to variations in the composition of shells beyond the first, as is clear from Eq. (5). The LCM performs rather well

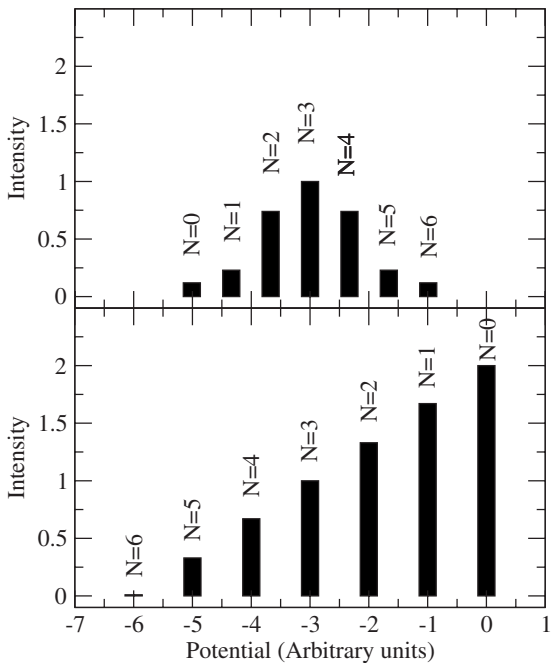

FIG. 3. Lower panel: schematic representation of the change in anion core-level XPS spectrum with variation in global anion composition (and hence average value of N_1). Upper panel: schematic representation of the contribution to the anion core XPS spectrum for 50/50 composition by sites with particular values of N_1.

for the close-packed fcc system but less so for more open lattices as has been pointed out previously.[8,28] One feature of Eqs. (5) and (7) that is not widely appreciated is emphasized in Fig. 3. Here the average A site potential is shown for an alloy with composition $A_{0.5}B_{0.5}$. Perhaps contrary to expectation, the effect of increasing the local B concentration (while preserving c_B) shifts the A site potential in the opposite direction to the shift in $\langle V\rangle$ caused by increasing the global B concentration. It is clear that this effect must be accounted for when using photoelectron energies to select specific local environments, for example, as in Auger-photoelectron coincidence spectroscopy.[20,21]

As has been discussed in detail previously[8] the LCM reproduces the *ab initio* Q-V_M properties of disordered alloys rather well, particularly for close-packed systems, and we may conclude that the model offers valid insight into electronic redistribution upon alloy formation. Agreement with *ab initio* results is semiquantitative for the body-centered-cubic $Cu_{0.5}Zn_{0.5}$ alloy as summarized in Table I. Writing

$$aQ^i + V_M^i = k, \tag{9}$$

we see that the Q-V_M gradient and intercept values, a and k, respectively, predicted by the LCM have magnitudes which are significantly too low, while the standard deviation of the charge distribution is significantly too large. We now consider a number of refinements to the LCM.

B. Multishell model

The limited success of the LCM when applied to more open lattices suggests a need to account for more influential

TABLE I. Q-V_M properties for Cu sites in the body-centered-cubic $Cu_{0.5}Zn_{0.5}$ alloy as deduced from *ab initio* calculations (Ref. 26) along with corresponding results obtained using the LCM [Eq. (4)], the multishell model [Eq. (10)] with optimized λ coefficients and β_{max} ranging from 2 to 5, and the electronegativity model (EM) [Eqs. (19) and (20)] with (η=0.06 and 0.09). All the model calculations assume an average charge of $-0.1e$ (as obtained from the *ab initio* calculations in Ref. 26).

	σ_Q	Q-V_M gradient	Q-V_M intercept
Ab initio[a]	0.026	25.0	−2.00
LCM	0.035	17.3	−1.17
O2-LCM	0.028	21.7	−1.63
O3-LCM	0.026	23.5	−1.82
O4-LCM	0.025	25.0	−1.98
O5-LCM	0.025	25.0	−1.98
EM(η=0.06)	0.027	25.1	−2.00
EM(η=0.10)	0.023	28.9	−2.20

[a]Reference 26.

neighbors beyond the first coordination shell, and this can be achieved using expressions of the form,

$$Q^i = 2S_0 \sum_{\beta=1}^{\beta_{max}} \lambda_\beta N_\beta^i. \tag{10}$$

Equation (10) leads to the site potentials,

$$V(N_1,N_2,N_3,N_4,\ldots) = \frac{2S_0}{R} \sum_{\beta=1}^{\beta_{max}} \lambda_\beta \sum_{\alpha=0}^{\infty} [Z_\alpha(1-c_0) - N_\alpha] f_\alpha(\beta), \tag{11}$$

with conditional averages,

$$\langle V \rangle = \frac{2S_0}{R}(1-c_0)(\rho_0^{-1}-1) \sum_\beta \lambda_\beta Z_\beta, \tag{12}$$

and variance,

$$\sigma_V^2 = \frac{4c_0(1-c_0)}{R^2} \sum_{\alpha=1}^{\infty} \left[\sum_{\beta=1}^{\beta_{max}} f_\alpha(\beta)\lambda_\beta \right]^2 Z_\alpha. \tag{13}$$

To investigate the effect of the second shell term while maintaining constant conditionally averaged charges, it is useful to rewrite Eq. (10) in the form,

$$Q^i = \frac{\langle Q \rangle}{(1-c_0)} \frac{\sum_{m=1}^{\beta_{max}} N_m \lambda_m}{\sum_{m=1}^{\beta_{max}} Z_m \lambda_m}, \tag{14}$$

where $\langle Q \rangle$ is the average charge of the species at site i, setting β_{max}=2. Q-V_M results for the body-centered-cubic lattice with $\langle Q \rangle$=−0.1 and λ_2/λ_1=0.01 and 0.02 are shown in Fig. 4. Introduction of the second shell term is seen to have a number of favorable consequences: the distribution of site charges becomes less discrete and with a lower variance,

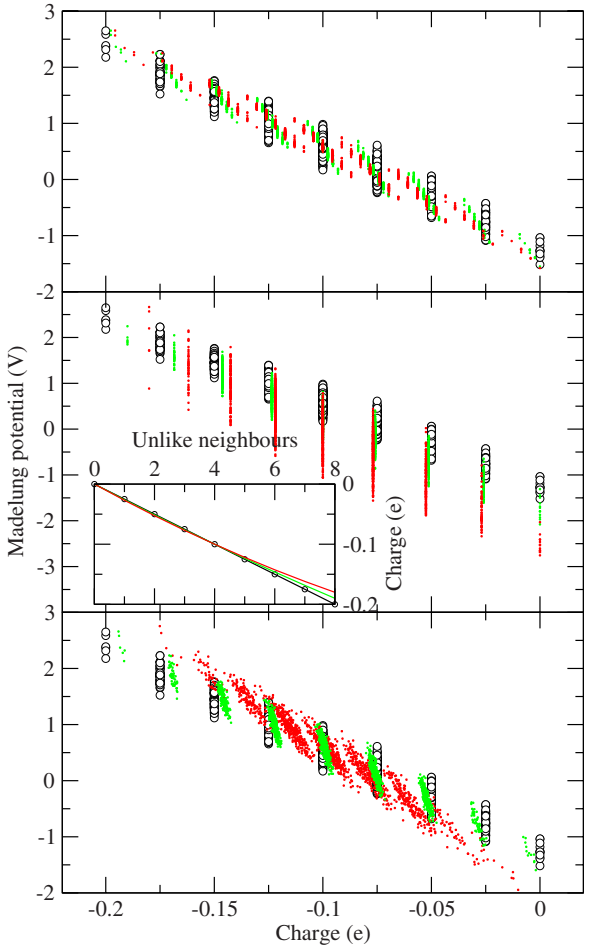

FIG. 4. (Color online) Madelung potential vs Q for the body-centered-cubic lattice. Upper panel: the two-shell model with λ_2/λ_1=0.0 (open circles), λ_2/λ_1=0.01 [green (light gray)], and λ_2/λ_1=0.02 [red (dark gray)]. Middle panel: the quadratic model (18) with μ=0 (open circles), 0.15 [green (light gray)], and 0.3 [red (dark gray)]. The inset shows the dependence of charge on number of unlike neighbors for each value μ. Lower panel: the electronegativity model with η=0.0 (open circles), η=0.03 [green (light gray)], and η=0.09 [red (dark gray)].

and the Q-V_M data set becomes more linear and with slightly increased gradient. While each of these observations indicates improved Q-V_M properties relative to the LCM, it is not clear *a priori* what are the appropriate values for the λ parameters and β_{max} in Eq. (10). One answer to this question is those values which lead to the most linear Q-V_M behavior. Since Q in Eq. (10) is independent of N_j for $j > \beta_{max}$ we now average over the occupations of shells beyond the β_{max}^{th} in Eq. (11) to obtain $\langle V(N_1,N_2,\ldots,N_{\beta_{max}}) \rangle$. It can then be shown that linearity of $\langle V(N_1,N_2,\ldots,N_{\beta_{max}}) \rangle$ in Q requires that the λ parameters form an eigenvector of the f matrix. The optimized two-shell linear charge model (O2-LCM) requires

$$f_1(2)\left(\frac{\lambda_2}{\lambda_1}\right)^2 + [f_1(1)+f_2(2)]\frac{\lambda_2}{\lambda_1} - f_2(1) = 0, \tag{15}$$

yielding λ_2/λ_1=0.22, 0.55, and 0.17 for the simple, body-centered, and face-centered lattices, respectively. When such

"optimized" λ parameters are adopted the gradient and intercept of the Q-V_M line (i.e., a and k in Eq. (9)) are then given by

$$a = \frac{1}{R}\left[2 + \sum_{\beta=1}^{\beta_{\max}} \frac{\lambda_\beta}{\lambda_1} f_1(\beta)\right], \tag{16}$$

$$k = \frac{2S_0(1-c_0)}{R} \sum_{\beta=1}^{\beta_{\max}} \lambda_\beta \sum_{\alpha=0}^{\beta_{\max}} f_\alpha(\beta) Z_\alpha. \tag{17}$$

Q-V_M plots obtained from cluster calculations employing Eq. (10) with optimized parameters are shown in Table I for the body-centered-cubic lattice and in Fig. 2 for the simple cubic, body-centered-cubic, and face-centered-cubic lattices. For the simple cubic and face-centered-cubic lattices we find the Q-V_M data to be well converged for $\beta_{\max}=3$, whereas the bcc lattice requires $\beta_{\max}=4$. From Table I we see that the optimized multishell model with $\beta_{\max}=4$ reproduces the gradient and intercept of the Q-V_M line as well as the charge variance obtained from *ab initio* calculations[26] for $Cu_{0.5}Zn_{0.5}$ when $\langle Q\rangle$, the only free parameter, is set to the correct the value of 0.1. In fact the numerical study of Wolverton *et al.*[8] already demonstrated the success of the multishell generalization of Magri's LCM although this does not appear to have been widely appreciated. In that work *ab initio* Q-V_M results were fitted numerically to the model of Eq. (10) and λ parameters extracted. For the relatively small (a few hundred sites) supercells considered $\beta_{\max}=2$ and 3 were found to be adequate for the face-centered-cubic and body-centered-cubic lattices, respectively.[8] Very similar values for the λ parameters were derived from the numerical fitting as found here by means of the optimized analytical procedure described above.

C. Nonlinear models

Having considered the role of multiple shells within a linear framework we now consider nonlinear behavior but limited to the first-neighbor shell. It is reasonable to suppose that the enthusiasm of an atom to exchange charge with its unlike neighbors will decrease with N_1, and indeed the dependence of atomic electronegativity on charge state is well known to chemists.[29] For bcc $A_{0.5}B_{0.5}$ alloys Eq. (4) can be modified to account for such behavior as follows:

$$Q^i = 2\lambda_1 N_1 S_0[1 - \mu(N_1 - 4)/12], \tag{18}$$

where the μ parameter lies in the interval [0,1], the upper limit ensuring the magnitude of Q increases monotonically with N_1. Q-V_M results obtained from cluster calculations employing two distinct values of μ are shown in the middle panel of Fig. 4. It is seen that even mild modification of the Magri charge law provokes considerable Q-V_M scatter.

An unfavorable feature of Eq. (18) is that, unlike the LCM, it does not guarantee local charge neutrality. A slightly more subtle generalization of Eq. (4) that does not suffer from this deficiency can be written as[12,28]

$$Q^i = \sum_{j \in nn^i} (\chi^j - \chi^i), \tag{19}$$

where

$$\chi^i = -S^i\lambda_1 + \eta Q^i, \tag{20}$$

with $S^i = \pm 1$ according to the species at site i. The difference $\chi^i - \chi^j$ can be thought of as the electronegativity difference between the two sites, a quantity which has been used successfully to model the vibrational entropy of alloys.[30] Substituting Eq. (20) into Eq. (19) yields

$$Q^i(1 + Z_1\eta) - \eta \sum_{j \in nn^i} Q^j = 2\lambda_1 N_1 S^i, \tag{21}$$

which has the form,

$$\Lambda^{ij} Q^j = 2\lambda_1 N_1 S^i, \tag{22}$$

and can be solved iteratively or else by explicit inversion of the Λ matrix. While the right-hand side of the previous equation is the LCM charge vector, the Λ matrix is determined by η and the lattice structure; in particular it is independent of the site occupations. Furthermore the matrix is sparse and very simple: when periodic boundary conditions are imposed, the matrix elements Λ_{ij} adopt only two distinct values: $1+Z_1\eta$ when $i=j$ and $-\eta$ when sites i and j are nearest neighbors. Thus Λ takes block circulant Toeplitz form and can be inverted analytically,[31,32] elements of the inverse are essentially exponentially decaying with distance from the diagonal.[32,33]

Results of cluster calculations employing Eqs. (19) and (20), the "electronegativity model (EM)," are shown in Fig. 4. For each value of η used a constant average charge $\langle Q\rangle$ was maintained by renormalizing λ_1 as follows:

$$\lambda_1 = \frac{\langle Q\rangle}{2(1-c_0)Z_1}(1 + \eta Z_1). \tag{23}$$

It can be seen that introduction of nonzero η in Eqs. (19) and (20) leads to qualitatively similar behavior to that obtained from the two-shell model (i.e., an improvement over the LCM). Although Table I shows that $\eta=0.06$ gives a rather good description of σ_Q as well as the Q-V_M gradient and intercept, it is clear from Fig. 4 that the Q-V_M data points do not form a satisfactory line even for 0.09. Slightly improved linearity is obtained for $\eta=0.1$ but at the expense of spoiling σ_Q, a, and k, as Table I shows. While alternative forms of nonlinear response can be imagined, the results described above, together with those obtained for the multishell model, suggest that nonlinear effects are not of major consequence in metallic alloys.

IV. DISCUSSION

In Secs. II and III we have pursued charged ball models and point-charge electrostatics in the belief that these can provide a framework for meaningful analysis of experimental electron spectroscopy measurements of disordered systems. Even within this limited context, however, it is not clear *a priori* that any model which collapses electronic

structure to a single number, Q^i, per site can have any connection with real alloys. On the other hand the *ab initio* Q-V_M laws are suggestive of some underlying simplicity. Indeed the coarse mesh Thomas-Fermi model proposed by Pinski[27] appears to capture the essential physics—it reproduces semiquantitatively the Q-V_M features of *ab initio* results and explains the apparent success of Magri-type charge models. The status of the Q-V_M "laws" was reinvestigated more recently in some detail by Ruban and Skriver (RS) (Ref. 23) using the locally self-consistent Green's-function (LSGF) method,[34] essentially a hybrid of the *ab initio* supercell and effective-medium approaches. From a large set of calculations involving different chemical species, crystal structures, and compositions, RS made a number of intriguing observations:

(i) $\langle Q\rangle/Q_{\rm SS}$, where $Q_{\rm SS}$ are the charges obtained from a conventional single-site CPA calculation, is a universal constant.

(ii) When charges and Madelung potentials are suitably normalized, a linear relationship holds with universal coefficients,

$$\frac{V_M^i R_{\rm WS}}{Q_{\rm SS}e^2} = \frac{Q^i}{Q_{\rm SS}}\gamma + \beta, \tag{24}$$

where $R_{\rm WS}$ is the Wigner-Seitz radius.

(iii) the single-site CPA charges and Madelung potentials also fall on the same Q-V_M line.

RS were able to explain these observations in terms of universal screening of charges in metallic alloys. In this regard it is instructive to consider the impurity limit. In the LCM the charge of an impurity site is screened by an opposing counter charge evenly distributed across the nearest-neighbor shell. Denoting the induced charge on a site in the mth nearest-neighbor shell, normalized to the impurity charge as ϕ_m, we have $\phi_1=-1/Z_1$ and $\phi_{m>1}=0$ in the LCM. For the multishell model we have $\phi_m=-\lambda_m/\Sigma_{\beta=1}^{\beta_{\rm max}} Z_\beta \lambda_\beta$. Values of ϕ_m for the simple cubic, body-centered-cubic and face-centered-cubic lattices derived from the optimized multishell model with $\beta_{\rm max}=5$ are shown in Fig. 5. The data points for the three structures appear to fall on a common curve and indicate some spilling of the screening charge beyond the nearest-neighbor shell, particularly for the bcc lattice where the second shell is relatively close to the first. We find excellent agreement with the charge redistributions previously observed in the Thomas-Fermi results in Ref. 27 for an impurity in a bcc host, also shown in Fig. 5. The electronegativity model of Eq. (19) gives similar behavior. The universal ϕ function deduced by RS (Ref. 23) from *ab initio* calculations for a variety of impurities and hosts with a variety of crystal structures and lattice parameters is shown by the dotted line in Fig. 5. Although lacking the Friedel oscillations (in fact it appears to have Yukawa form with range $\sim R_{\rm WS}/2$), the empirical ϕ obtained from the multishell model can be seen to provide a reasonable approximation to the *ab initio* function.

By considering the modification of site charges in a random alloy when a single atom is substituted for one of the opposite chemical type, RS also investigated charge screening in alloys away from the dilute limit. They found that the universal screening function illustrated in Fig. 5 holds across the composition range and therefore so should the parallel with the multishell model. Furthermore it was pointed out some time ago[11,23] that while the Magri LCM can be invoked on the basis of "chemical intuition," it can also be derived from the assumption of universal first-neighbor screening. The same argument holds for the multishell model as follows. At A (B) sites we place a charge $\bar{Q}_A(\bar{Q}_B)$ and then distribute a countercharge on the neighboring sites with relative weights given by the universal screening function. The resulting site charges are

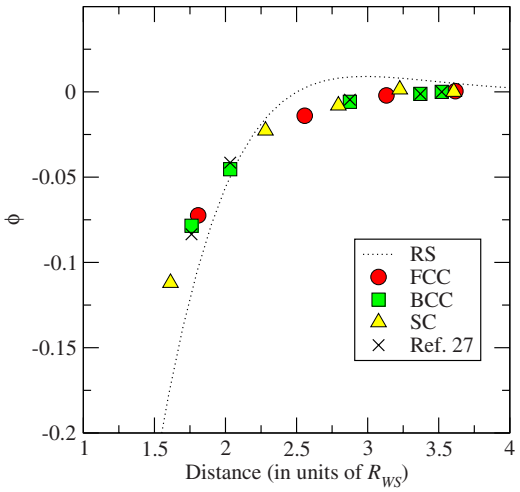

FIG. 5. (Color online) Induced site charges, ϕ, normalized to the impurity charge around an impurity in fcc (circles), bcc (squares), and sc (triangles) hosts. The crosses represent corresponding results from Ref. 27 for an impurity in a bcc host. The dotted curve illustrates the universal screening function obtained in Ref. 23. The symbols correspond to λ parameters obtained from the optimized multishell model [Eq. (10)].

$$Q^i = \bar{Q}_A\delta_{iA} + \bar{Q}_B\delta_{iB} - \sum_{m=1}^{\infty}\phi_m\sum_{j\in m}[\bar{Q}_A\delta_{jA} + \bar{Q}_B\delta_{jB}] \tag{25}$$

$$= \frac{\langle Q\rangle}{1-c_0}\sum_{m=1}^{\infty}\phi_m N_m. \tag{26}$$

This expression has precisely the form of the multishell model in Eq. (14) with parameters λ_m/λ_1 given by ϕ_m/ϕ_1. In fact we find that a multishell model with parameters fixed by the RS screening function gives poorer Q-V_M properties than the LCM. We must conclude that the superposition argument implicit in Eq. (25), although a good approximation, is not perfect. For the same reason the multishell model with optimized Q-V_M properties yields only an approximate screening function. Insightful discussion of the fundamental link between screening in alloys and Magri-type charge models can also be found in Refs. 8, 9, and 27.

While models such as the LCM seek to predict the site charges in solids on the basis of some simple and plausible rule, a more satisfying framework would allow site charges

to emerge from a variational treatment of the total energy, as in the electron-gas model in Ref. 27. Such a charged ball model can be constructed by adding the Madelung energy of the system to the energy cost of charging the balls,

$$E = \sum_i E_i^{\text{local}} + E^M m \tag{27}$$

$$= a_A \sum_{i=A} Q^i (Q^i - \gamma_A) + a_B \sum_{i=B} Q^i (Q^i - \gamma_B) + \sum_i Q^i V_M^i / 2, \tag{28}$$

where the total energy of a free ion has been expressed as a second-order Taylor expansion in Q. In principle the atomic constants a_A, a_B, γ_A, and γ_B can be derived from Hartree-Fock calculations for free ions or even experimental ionization potential and electron affinity measurements. Making the uniform charge assumption the model becomes trivial—the Madelung energy vanishes and there is only a single variational parameter, Q_A^{UCA}. The total energy, E^{UCA}, and the A and B charges, Q_A^{UCA} and Q_B^{UCA}, are easily expressed in terms of the atomic constants and the "true" total energy can then be rewritten as

$$E - E_{\text{UCA}} = a_A \sum_{i=A} (Q^i - Q_A^{\text{UCA}})^2 + a_B \sum_{i=B} (Q^i - Q_B^{\text{UCA}})^2 + E_M. \tag{29}$$

In fact this expression was derived by Bruno, Zingales, and Wang (BZW) (Ref. 24) not from the atomic perspective but motivated by the RS universal screening function and the observation that the interaction between a site charge and its screening charge can be thought of essentially as an intrasite energy. Drchal *et al.*[25] showed that the BZW model implies an exactly linear Q-V_M relationship and that model parameters appropriate for real alloys reproduce the RS screening function rather well.

Finally we turn to core-level x-ray excited photoelectron spectroscopy (XPS) simulations. Aside from intracore terms which are independent of chemical environment, core-level eigenvalues are given by Eq. (1). Neglecting relaxation energy shifts, we can write the photoelectron spectrum of a particular core level of a disordered alloy as

$$I(\omega) = G_{\sigma_E}(\omega) \otimes \left[\sum_i L_\Gamma(\omega - V^i) \right] \approx G_{\sigma_E}(\omega) \otimes L_\Gamma(\omega - \langle V \rangle) \otimes G_{\sigma_V}, \tag{30}$$

where G_{σ_E} is the Gaussian function with standard deviation σ_E representing instrumental broadening (the experimental resolution corresponding to $2.35\sigma_E$), L_Γ is a Lorentzian with width Γ representing lifetime broadening, and $\otimes$ indicates the convolution operator. Surface core-level shifts, Doniac-Sunjic asymmetry, and inelastic scattering can all be accounted for in analysis of experimental alloy spectra[12] but are inessential complications presently. Spectra obtained from Eq. (30) using the LCM and O5-LCM are shown in Fig. 6. In each case the values $\Gamma = 0.60$ eV, $\sigma_E = 0.13$ eV, and $\langle Q \rangle = -0.1$ have been assumed, corresponding to measurement of the Cu $2p_{3/2}$ core line of $Cu_{0.5}Zn_{0.5}$ with a high-resolution XPS spectrometer. For comparison $G_{\sigma_E} \otimes L_\Gamma$ is also shown to represent the core spectrum of an ordered system. It can be seen that both LCM and O5-LCM calculations predict a strong disorder broadening effect which should be easily measurable. In fact previous experimental[14] and *ab initio* computational[17] results for $Cu_{0.5}Zn_{0.5}$ found $\sigma_V = 0.09$ and 0.15 eV, respectively, suggesting that the LCM (which gives $\sigma_V = 0.26$ eV) significantly overestimates the disorder broadening of core-level binding energies. Generalization to O5-LCM appears to make the disagreement worse. The implication is that modeling experimental core disorder broadening measurements by means of the LCM or O5-LCM would lead to gross overestimates of the free parameter in these models (i.e., λ_1 or $\langle Q \rangle$).

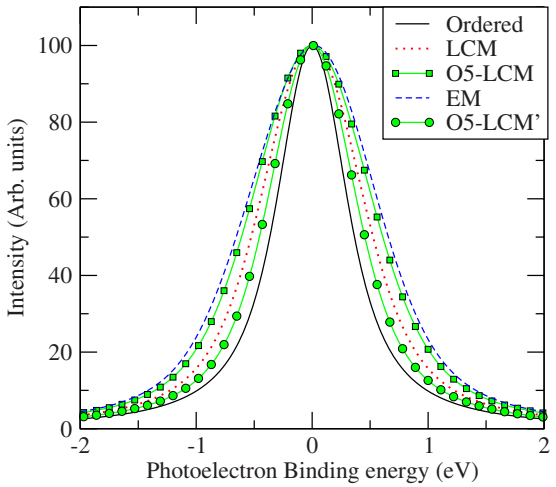

FIG. 6. (Color online) XPS simulations using the LCM, multishell model, and the EM.

In seeking to understand the differences between the LCM and O5-LCM spectra and to explain their apparent overestimating of core disorder broadening, observed also for other alloys,[12,13] it is instructive to consider separately the contributions arising from variations in V_{ia} and V_M. In fact it can be shown that the variance of the Madelung potential differs very little between LCM (0.396 eV^2) and O5-LCM (0.388 eV^2). O5-LCM gives better Q-V_M behavior than LCM by virtue of reducing the charge variance, as shown in Table I, with the direct effect of reducing the variance in V_{ia} and therefore of increasing σ_V^2. Since we know that O5-LCM (and to a lesser extent LCM) give a very good description of both σ_Q^2 and $\sigma_{V_M}^2$, we must attribute our difficulties with σ_V^2 to the failure of the assumed form of the intra-atomic potential, $V_{ia}^i = Q^i/\rho_0 R = 2Q^i/R$. This expression follows from a literal picture of close-packed charged balls with excess charge residing at their surfaces, but ideally one would prefer a model of V_{ia} based upon a knowledge of the expectation value $\langle 1/r \rangle$ for the local charge density of real solids. Certainly *ab initio* calculations could be used to guide the choice of ρ_0. In this context it is worth noting that Faulkner *et al.*[17] found that for $Cu_{0.5}Zn_{0.5}$ the *ab initio* core eigenvalues and site potentials determined by Eq. (1) appear to be perfectly linearly correlated but with gradient $\delta\epsilon/\delta V \approx 0.55$ rather than 1. Decreasing ρ_0 from its assumed value of 1/2 to 1/3 (the value obtained when the excess charges are uniformly dis-

tributed throughout balls of radius $R/2$) would bring $\delta\epsilon/\delta V$ and σ_V^2 from the O5-LCM into agreement with *ab initio* results.[17] The O5-LCM XPS simulation assuming $\rho_0=1/3$ is also shown in Fig. 6. The disorder broadening effect of the core-level photoelectron spectrum is much reduced and now agrees with Ref. 17.

Experimental photoelectron spectroscopy has revealed core disorder broadening in $Cu_{0.5}Zn_{0.5}$ with standard deviation 0.09 eV,[14] somewhat less than that predicted by *ab initio*[17] and O5-LCM calculations. Likely explanations for this observation are (i) the possibility of short-range order in the samples studied experimentally and (ii) a final-state disorder broadening effect that tends to cancel σ_V. The latter can arise because the core photoemission process leaves an atom with a core hole causing substantial local relaxation of the charge density. Marten *et al.*[18] found that, like the ground-state core potential V, the relaxation energy varies with local environment in disordered alloys.

V. SUMMARY

The LCM is reasonably self-consistent in the sense that the Madelung potentials it implies are determined almost completely by the local composition, as were the charges that created them. The model leads to a good (although not perfect) representation of the Q-V_M behavior computed by *ab initio* electronic structure calculations. It is reasonable to expect that a charge law that better reflects variation in the local environment would give improved Q-V_M performance. To this end two generalizations of the LCM have been considered, each representing a distinct physical effect. An electronegativity model in which charge is exchanged between unlike nearest neighbors in a nonlinear fashion yielded improved sets of charges and potentials but Q-V_M pairs did not approach a strictly linear relationship. A linear multishell model on the other hand was able to reproduce *ab initio* Q-V_M behavior extremely well and implied a universal screening function rather similar to that discovered by Ruban and Skriver.[23] While the model allows an excellent description of Madelung potential in disordered alloys the intra-atomic contribution to the potential seen by core electrons is specified only semiquantitatively. It is hoped that *ab initio* calculations can be used to substantiate the empirical result (i.e., $\rho_0 \sim 1/3$) found here.

[1] N. W. Ashcroft and N. D. Mermin, *Solid State Physics* (Saunders College, Philadelphia, 1976).
[2] B. L. Gyorffy, D. D. Johnson, F. J. Pinski, D. M. Nicholson, and G. M. Stocks, in *Alloy Phase Stability*, edited by G. M. Stocks and A. Gonis (Plenum, New York, 1994), p. 293.
[3] D. D. Johnson, D. M. Nicholson, F. J. Pinski, B. L. Gyorffy, and G. M. Stocks, Phys. Rev. Lett. **56**, 2088 (1986).
[4] D. D. Johnson, D. M. Nicholson, F. J. Pinski, B. L. Gyorffy, and G. M. Stocks, Phys. Rev. B **41**, 9701 (1990).
[5] I. A. Abrikosov and B. Johansson, Phys. Rev. B **57**, 14164 (1998).
[6] R. Magri, S. H. Wei, and A. Zunger, Phys. Rev. B **42**, 11388 (1990).
[7] C. Wolverton and A. Zunger, Phys. Rev. B **51**, 6876 (1995).
[8] C. Wolverton, A. Zunger, S. Froyen, and S. H. Wei, Phys. Rev. B **54**, 7843 (1996).
[9] D. D. Johnson and F. J. Pinski, Phys. Rev. B **48**, 11553 (1993).
[10] I. A. Abrikosov, Yu. H. Vekilov, P. A. Korzhavyi, A. V. Ruban, and L. E. Shilkrot, Solid State Commun. **83**, 867 (1992).
[11] P. A. Korzhavyi, A. V. Ruban, I. A. Abrikosov, and H. L. Skriver, Phys. Rev. B **51**, 5773 (1995).
[12] R. J. Cole, N. J. Brooks, and P. Weightman, Phys. Rev. Lett. **78**, 3777 (1997).
[13] R. J. Cole and P. Weightman, J. Phys.: Condens. Matter **10**, 5679 (1998).
[14] D. Lewis, R. J. Cole, and P. Weightman, J. Phys.: Condens. Matter **11**, 8431 (1999).
[15] A. W. Newton, A. Vaughan, R. J. Cole, and P. Weightman, J. Electron Spectrosc. Relat. Phenom. **107**, 185 (2000).
[16] A. W. Newton, S. Haines, P. Weightman, and R. J. Cole, J. Electron Spectrosc. Relat. Phenom. **136**, 235 (2004).
[17] J. S. Faulkner, Y. Wang, and G. M. Stocks, Phys. Rev. Lett. **81**, 1905 (1998).
[18] T. Marten, W. Olovsson, S. I. Simak, and I. A. Abrikosov, Phys. Rev. B **72**, 054210 (2005).
[19] P. Weightman, Rep. Prog. Phys. **45**, 753 (1982).
[20] Z.-T. Jiang, S. M. Thurgate, G. van Riessen, P. Wilkie, and C. Creagh, J. Electron Spectrosc. Relat. Phenom. **130**, 33 (2003).
[21] R. D. Stoker, M. Szmigiel, N. J. Miller, and R. J. Cole, J. Electron Spectrosc. Relat. Phenom. **162**, 127 (2008).
[22] G. G. Kleiman and R. Landers, J. Electron Spectrosc. Relat. Phenom. **88-91**, 435 (1998).
[23] A. V. Ruban and H. L. Skriver, Phys. Rev. B **66**, 024201 (2002).
[24] E. Bruno, L. Zingales, and Y. Wang, Phys. Rev. Lett. **91**, 166401 (2003).
[25] V. Drchal, R. Hammerling, and P. Weinberger, Phys. Rev. B **74**, 214202 (2006).
[26] J. S. Faulkner, Y. Wang, and G. M. Stocks, Phys. Rev. B **52**, 17106 (1995).
[27] F. J. Pinski, Phys. Rev. B **57**, 15140 (1998).
[28] R. J. Cole and P. Weightman, J. Phys.: Condens. Matter **9**, 5609 (1997).
[29] J. C. Phillips, Rev. Mod. Phys. **42**, 317 (1970).
[30] O. Delaire and B. Fultz, Phys. Rev. Lett. **97**, 245701 (2006).
[31] M. Dow, ANZIAM J. **44**, E185 (2003).
[32] G. Meurant, SIAM J. Matrix Anal. Appl. **13**, 707 (1992).
[33] R. Nabben, SIAM J. Matrix Anal. Appl. **20**, 820 (1999).
[34] I. A. Abrikosov, A. M. N. Niklasson, S. I. Simak, B. Johansson, A. V. Ruban, and H. L. Skriver, Phys. Rev. Lett. **76**, 4203 (1996).